Identification of genes with therapeutic and prognostic values in lung adenocarcinoma microenvironment

Xueping Jiang
Department of Radiation and Medical Oncology, Zhongnan Hospital of Wuhan University
Yanping Gao
Department of Radiation and Medical Oncology, Zhongnan Hospital of Wuhan University
Nannan Zhang
Department of Radiation and Medical Oncology, Zhongnan Hospital of Wuhan University
Cheng Yuan
Department of Radiation and Medical Oncology, Zhongnan Hospital of Wuhan University
Yuan Luo
Department of Radiation and Medical Oncology, Zhongnan Hospital of Wuhan University
Wenjie Sun
Department of Radiation and Medical Oncology, Zhongnan Hospital of Wuhan University
Jianguo Zhang
Department of Radiation and Medical Oncology, Zhongnan Hospital of Wuhan University
Jiangbo Ren
Department of Biological Repositories, Zhongnan Hospital of Wuhan University
Yan Gong
Department of Biological Repositories, Zhongnan Hospital of Wuhan University
Conghua Xie (chxie_65@whu.edu.cn)
Department of Radiation and Medical Oncology, Zhongnan Hospital of Wuhan University
https://orcid.org/0000-0001-6623-9864

Research

Keywords: Lung adenocarcinoma, Tumor microenvironment, Therapeutic values, Prognosis, Biomarker

Posted Date: March 12th, 2020

DOI: https://doi.org/10.21203/rs.3.rs-16969/v1

Abstract

Background

As the most diagnosed malignancy, lung cancer is also the primary cause of cancer death in the entire world. The therapy of lung adenocarcinoma (LUAD), which is the most prevalent subtype of lung cancer, draw researchers' increasing attentions. This research aimed to investigate the tumor microenvironment (TME)-related hub genes which might be novel targets for treatment.

Materials and methods

LUAD-associated data packages, including RNA-Seq information and clinical data of 522 patients, were obtained from The Cancer Genome Atlas (TCGA). For better evaluation of stromal and immune cell components, immune scores, stromal scores and estimate scores were obtained with ESTIMATE algorithm based on gene expression levels in tumors. The R package heatmap and clustering analysis were used to explore interested genes. Differentially expressed genes (DEGs) were identified by Venn diagram. Protein-protein interaction (PPI) network was applied to explore intrinsic connections of DEGs. Kaplan-Meier (K-M) survival curves, Gene Ontology (GO) and Kyoto Encyclopedia of Genes and Genomes (KEGG) analysis were applied to investigate the prognostic values and intricate biological functions of DEGs. The relationships between 4 survival-related hub genes and 6 types of immune cells were examined using TIMER database. The LinkedOmics database was applied to look for kinase targets of hub genes.

Results

The immune/stromal/estimate scores were significantly correlated with clinical features, including the grades and sizes of LUAD, distant metastasis and outcomes. A total of 702 DEGs, 589 up-regulated and 113 down-regulated, were identified. GO and KEGG analysis showed that the DEGs had significant correlations with tumor immunology. PPI network suggested that the top 8 nodes were FPR2, C3AR1, MCHR1, CCR5, FPR1, CCL19, CCR2 and CXCL10. K-M survival curves indicated that FPR2, C3AR1, MCHR1 and CCR5, as hub genes, were significantly correlated with the overall survival (OS) of LUAD patients. The expression levels of C3AR1 and CCR5 were positively correlated with immune cell infiltration. LYN, LCK and SYK were the targeted kinases of these hub genes.

Conclusion

FPR2, C3AR1, MCHR1 and CCR5 were TME-related genes and potential biomarkers for the therapy and prognosis of LUAD.

Introduction

Lung cancer is the most frequent malignant carcinoma, and also the major cause of cancer death[1]. Base on histopathologic characteristics, non-small cell lung cancer (NSCLC) accounts for approximately

85% of all lung cancer, and lung adenocarcinoma (LUAD) is the major component of NSCLC[2]. While LUAD patients benefited from multiple treatments, including radiotherapy, chemotherapy and immunotherapy, the 5-year survival rate was still under 20%[3]. Therefore, it is eager to identify novel biomarkers to raise the curative rates, reduce the death rates and improve survival quality.

Tumor microenvironment (TME) composes of cells (endothelial cells, neuroendocrine cell and immune cells, etc.) and extracellular components (cytokines, chemokines and extracellular matrix, etc.). TME has significant effects on the initiation, development, metastasis, and recurrence of carcinoma[4, 5]. It was reported that TME affected gene expression, such as SDF1[6] and CXCR4[7]. Emerging evidence showed that regulation of TME facilitated chemotherapy and immunotherapy to improve the prognosis of patients[8]. It is vital to find TME-related genes to increase the efficiency of therapies.

As the essential ingredients of TME, immune and stromal cells play substantial effects on signal transduction, immune surveillance and immune scape[9, 10]. To accurately evaluate the percentage of immune and stromal cells in tumors, Yoshihara et al. obtained scores for tumor purity, the infiltration levels of immune cells and stromal cells in tumor tissues based on gene expression levels using ESTIMATE algorithm[11]. Precious studies also suggested that TME-related biomarkers were helpful in histological diagnosis and prognostic prediction using big-data based ESTIMATE algorithm[12, 13].

As a publicly available database, The Cancer Genome Atlas (TCGA) includes abundant cancer-causing genomic alterations data of more than 30 human tumor types[14]. In the current study, we obtained transcription profiles and clinical information of LUAD patients, including ages, genders, tumor stages, survival states and prognosis from TCGA database. The immune and stromal scores were calculated, and specific gene expression signatures of immune and stromal cells were analyzed. TME-related prognostic genes were identified, and the correlations between hub genes and immune cell infiltration were explored. The kinase targets of hub genes were also screened.

Materials And Methods

Data collection and preprocessing

The transcription profiles and clinical data of 522 LUAD patients were obtained from TCGA GDC website (http://portal.gdc.cancer.gov/)[14]. Normalization process was carried out with the R package limma[15]. Using ESTIMATE algorithm, the immune scores, stromal scores and estimate scores were calculated.

Screening of differentially expressed genes

Bioconductor limma package was applied to screen differentially expressed genes (DEGs) from the immune and stromal score groups. $|\log(FC)| > 1$ and False Discovery Rate (FDR) < 0.05 were set as the cutoffs to screen DEGs[15].

Heatmap and clustering analysis

R package heatmap and clustering analysis were used to obtain up- and down-regulated genes in the immune and stromal score groups, respectively[16]. Venn diagram package in R software was used to obtain the up- and down-regulated genes in both the immune score group and stromal score group[17]. The total overlapping DEGs were retained for subsequent analysis.

Functional and signal pathways enrichment analysis

The GO and KEGG analysis were applied to explore the function of DEGs. GO analysis included 3 parts: biological processes (BPs), molecular functions (MFs) and cellular components (CCs). To make data visible, 4 R packages, clusterProfiler, org.Hs.eg.db, enrichplot and ggplot2, were applied[18], and the top 10 enrichment clusters were shown in the bar charts. KEGG analysis was shown in the bubble chart. $P < 0.05$ and $q < 0.05$ were defined as cut-offs criterion.

Construction of protein-protein interaction network and overall survival curve

STRING (https://string-db.org/) was applied to construct protein-protein interaction (PPI) network[19], with the consideration of 0.9 as minimum interaction score. Overall survival (OS)-related hub genes were analyzed with K-M Plotter (http://kmplot.com/analysis/)[20].

Immune infiltration in TME

TIMER (https://cistrome.shinyapps.io/timer/) was used to investigate the interrelations between hub genes and 6 types of immune cells, including B cells, CD4 + T cells, CD8 + T cells, macrophages, neutrophils and dendritic cells[21].

Identified the kinase targets of hub genes

LinkedOmics database (http://www.linkedomics.org/) was used to explore the kinase targets of hub genes[22]. $P < 0.05$ was considered as statistical significance.

Results

Data source and clinical characteristics

The 522 LUAD patient's clinical data and profiles of 60483 mRNA expression were downloaded from TCGA database in February 2020. The clinical characteristics of LUAD patients were exhibited in Table 1.

Table 1
Clinical characteristics of 522 LUAD patients from TCGA cohort

	Male (%)	Female (%)	Total (%)
Sex	242 (46.4%)	280 (53.6%)	522 (100.0%)
Age (years)			
≤ 65	110 (21.9%)	131 (26.0%)	241 (47.9%)
> 65	123 (24.5%)	139 (27.6%)	262 (52.1%)
Status			
Dead	80 (15.3%)	87 (16.7%)	167 (32.0%)
Alive	162 (31.0%)	193 (37.0%)	355 (68.0%)
TNM stage*			
I	163 (31.7%)	116 (22.6%)	279 (54.3%)
II	56 (10.9%)	68 (13.2%)	124 (24.1%)
III	46 (8.9%)	39 (7.6%)	85 (16.5%)
IV	12 (2.3%)	14 (2.7%)	26 (5.1%)
T*			
1	61 (11.7%)	111 (21.4%)	172 (33.1%)
2	143 (27.5%)	138 (26.6%)	281 (54.1%)
3	27 (5.2%)	20 (3.9%)	47 (9.1%)
4	10 (1.9%)	9 (1.8%)	19 (3.7%)
N*			
0	150 (29.4%)	185 (36.3%)	335 (65.7%)
1	53 (10.4%)	45 (8.8%)	98 (19.2%)
2	36 (7.1%)	39 (7.6%)	75 (14.7%)
3	0 (0%)	2 (0.4%)	2 (0.4%)
M*			
0	172 (45.5%)	181 (47.9%)	353 (93.4%)
1	14 (3.7%)	11 (2.9%)	25 (6.6%)
*Partial missing of clinical characteristics.			

The immune and stromal scores associated with LUAD clinical features

In the LUAD patients database, the immune scores ranged from − 936.191 to 3453.015, the stromal scores ranged from − 1783.99 to 2107.561, and the ESTIMATE scores ranged from − 2344.43 to 4911.592. The immune scores (P = 0.03) and ESTIMATE scores (P = 0.048) were negatively correlated with stages (Fig. 1A). The lower immune scores (P = 0.003) and ESTIMATE scores (P = 0.028), the larger tumor sizes (Fig. 1B). However, there was no statistically significant difference between these scores and lymph node metastases (Fig. 1C). LUAD patients with distant metastases had lower stromal scores (P = 0.007) and ESTIMATE scores (P = 0.016, Fig. 1D).

According to median immune scores, LUAD patients were separated into low immune score cluster (n = 267) and high immune score cluster (n = 268). Based on median stromal scores, LUAD patients were also separated into low stromal score cluster (n = 267) and high stromal score cluster (n = 268). K-M survival curves showed that the high immune score group had longer OS than the low immune group (P = 0.021, Fig. 2A), and that the high stromal score group had longer OS than the low stromal group (P = 0.103, Fig. 2B). In addition, the high ESTIMATE score group had longer OS than the low ESTIMATE group (P = 0.034, Fig. 2C). These results exhibited that the immune and stromal scores were significantly associated with OS.

Screening DEGs based on immune/stromal scores

Limma package in R software was used to screen the DEGs in transcription profiles of LUAD samples from the high and low score groups. The heatmap based on immune scores exhibited 1092 up-regulated and 302 down-regulated genes (Fig. 3A). On the basis of stromal scores, we identified 1429 up-regulated genes and 211 down-regulated genes (Fig. 3B). Fold change (FC) > 2 and $p < 0.05$ were considered as criterion. Venn diagrams showed that the expression of 589 genes were up-regulated (Fig. 3C) and 113 genes were down-regulated (Fig. 3D). These 702 genes were defined as DEGs (Table S1) for subsequence analysis.

The roles of DEGs in the progression of LUAD

The GO and KEGG analyses were applied to explore the functions of these 702 DEGs. Top 10 DEGs of the BPs, CCs and MFs were shown in Fig. 4A. The enrichment of BPs mainly included the activation of cell surface receptor, adaptive immune response based on somatic recombination of immune receptors built from immunoglobulin superfamily domains, immune response mediated by lymphocytes, especially B cells, humoral immune response mediated by circulating immunoglobulin, complement activation and protein activation cascade. The top 10 enriched MFs included antigen binding, immunoglobulin receptor binding, immunoglobulin binding, carbohydrate binding, chemokine activity, chemokine receptor binding, cytokine receptor activity, cytokine activity, MHC protein binding and CCR chemokine receptor binding. The top 10 enriched CCs included T cell receptor complex, external side of plasma membrane, plasma membrane receptor complex, immunoglobulin complex and circulating, blood microparticle, tertiary granule membrane, tertiary granule, secretory granule membrane, specific granule membrane and specific

granule. The similar results were also observed in KEGG analysis (Fig. 4B). The consequence of KEGG enrichment was mainly associated with immune response signal pathways, such as cytokine-cytokine receptor interaction, chemokine signaling pathway and cell adhesion molecule (CAM), and NF-κB signaling pathway.

Integrated the interrelation of DEGs and identified significance genes

STRING method (https://string-db.org/) was used to construct a PPI network of the 702 DEGs, including 366 nodes and 637 edges, with the average node degree of 3.48 (Fig. 4C). The top 8 significant genes were FPR2, C3AR1, MCHR1, CCR5, FPR1, CCL19, CCR2 and CXCL10 (Fig. 4D).

Different roles of the hub genes in immune cell infiltration

The expression of FPR2, C3AR1, MCHR1 and CCR5 were significantly associated with the OS of LUAD patients (Fig. 5). These 4 genes were defined as hub genes. FPR1, CCL19, CCR2 and CXCL10 were not significantly associated with the OS of LUAD patients (Figure S1).

The online program TIMER was used to investigate the correlations between the hub genes and immune cells. Our results suggested positive correlations between the expression of C3AR1 and B cell, CD4 + T cell, CD8 + T cell, macrophage, neutrophil, and dendritic cell infiltration. The expression levels of CCR5 were also significantly correlated with immune cell infiltration. However, FPR2 and MCHR1 were only partially related with immune cell infiltration (Fig. 6).

Kinase targets of hub genes

LinkedOmics database includes miRNA targets, kinase targets and clinical features of 32 cancer types. It was used to explore the kinase targets of hub genes. The top 5 kinase targets of each hub gene were shown in Table 2. LYN, LCK and SYK were mutual kinase targets of hub genes (Figure S2).

Table 2

Kinase targets of hub genes.

Gene	Enriched kinase target	Description	Enrichment Score	LeadingEdgeNum
FPR2	Kinase_LYN	LYN proto-oncogene, Src family tyrosine kinase	0.807236557	22
	Kinase_LCK	LCK proto-oncogene, Src family tyrosine kinase	0.794046079	24
	Kinase_SYK	spleen associated tyrosine kinase	0.82327774	18
	Kinase_FYN	FYN proto-oncogene, Src family tyrosine kinase	0.749959628	28
	Kinase_ITK	IL2 inducible T-cell kinase	0.96610501	5
C3AR1	Kinase_LYN	LYN proto-oncogene, Src family tyrosine kinase	0.882421987	24
	Kinase_SYK	spleen associated tyrosine kinase	0.897063784	21
	Kinase_HCK	HCK proto-oncogene, Src family tyrosine kinase	0.890820109	9
	Kinase_LCK	LCK proto-oncogene, Src family tyrosine kinase	0.867567192	21
	Kinase_FYN	FYN proto-oncogene, Src family tyrosine kinase	0.817813149	19
MCHR1	Kinase_LYN	LYN proto-oncogene, Src family tyrosine kinase	0.811121472	24
	Kinase_SYK	spleen associated tyrosine kinase	0.790597866	17
	Kinase_LCK	LCK proto-oncogene, Src family tyrosine kinase	0.791580159	25
	Kinase_PRKCG	protein kinase C gamma	0.746655472	18
	Kinase_BTK	Bruton tyrosine kinase	0.912865896	4
CCR5	Kinase_LYN	LYN proto-oncogene, Src family tyrosine kinase	0.885105485	28
	Kinase_LCK	LCK proto-oncogene, Src family tyrosine kinase	0.892346921	22
	Kinase_SYK	spleen associated tyrosine kinase	0.896077906	18

Gene	Enriched kinase target	Description	Enrichment Score	LeadingEdgeNum
	Kinase_BTK	Bruton tyrosine kinase	0.966286502	4
	Kinase_HCK	HCK proto-oncogene, Src family tyrosine kinase	0.891136936	14

Discussion

Lung cancer draws more attention due to its substantial morbidity and mortality. The noteworthy features of lung cancer are fast development, highly malignant, low rates of early diagnosis, and adverse prognosis, seriously harming human health and wellbeing[1]. LUAD is the most prevalent subtype of lung cancer. During last decades, the discoveries of many therapy targets substantially improved the efficacy, including KRAS, EGFR, BRAF, ALK[23–25]. However, LUAD prognosis are still not satisfied. Our research aimed to screen and identify novel targets related to immune infiltration in TME.

The ESTIMATE algorithm was first proposed in 2013 by Yoshihara et al. This method helped researches to calculate 3 scores of tumor tissues, include estimate scores reflecting tumor purity, immune scores standing for immune cell infiltration and stromal scores inferring the presence of stroma. In our study, the 522 LUAD patients were divided into different groups: high immune/stromal groups and low immune/stromal groups. A total of 702 DEGs were identified, and the GO and KEGG analysis showed that these DEGs participated in inflammatory response, innate immune response, and adaptive immune response. In BPs, DEGs were mainly enriched in humoral immune response, the activation of cell surface receptor and complement. In MFs, potential pathways included the binding of antigen, immunoglobulin receptor, chemokine receptor, MHC protein and CCR chemokine receptor, the activity of chemokine, cytokine receptor and cytokine activity. In CCs, GO-enriched functions included immunoglobulin complex, T cell receptor complex. Similarly, KEGG analysis showed that DEGs were mainly enriched in signaling pathways related to B/T cell receptors, CAMs, and Chemokines. Some DEGs were also involved in the transductions of NF-κB signals and Toll-like receptor signals[26]. These results accorded with previous reports on the functions of immune and stromal cells in the TME of LUAD patients[27–29].

To analyze the inherent relations of DGEs, PPI analysis was performed by STRING tool, and the results showed that most DEGs participated in immune or inflammatory responses. We obtained the top 8 nodes, including FPR2, C3AR1, MCHR1, CCR5, FPR1, CCL19, CCR2 and CXCL10. Previous study showed that FPR2 deficiency increased secretion of CCL2 and facilitated M2 polarization of macrophages, promoting tumor progression[30]. In addition, FPR2 enhanced invasion and migration of cancer cells in gastric cancer and colorectal cancer[31, 32]. Mathern et al. found that T cell-expressed C3AR1 amplified the expression of antigen presenting cell costimulatory molecules and innate cytokines, promoting CD8 + T cell proliferation and expansion[33]. Moreover, C3A/C3AR1 signaling facilitated the lung metastasis via activating PI3K/AKT signaling pathway in breast cancer[34]. In gastric cancer, a combined treatment of anti-CCR5 and anti-PD1 improved CD4 + and CD8 + T cell infiltration and reduced the load of mice bearing

tumors[34]. The eutopic expression of CCR5 activated calcium signaling and enhanced Treg cell differentiation and infiltration[35]. Previous studies also showed that FPR1 deficient dendritic cells could not elicit anti-tumor T cell immunity, and that FPR1 was required in chemotherapy-induced anti-tumor immunity[36]. As a significant immune-related cytokine, CCL19 enhanced the development of an immune-stimulating intertumoral niche via increasing anti-tumorous CD8 + T cell accumulation in tumor tissues[37]. In hepatocellular carcinoma, knocking out of CCR2 suppressed the tumor progression via inhibiting infiltration and M2 polarization of macrophages, activating CD8 + T cells in TME[38]. K Au K et al. demonstrated that CXCL10 was a positive determinant of anti-tumor immune responses in high grade serous ovarian cancer. Overexpressed CXCL10 reduced tumor burden and the accumulation of malignant ascites, and increased CXCL10 expression resulted in IFN signaling pathway activation and increased expression of STAT1, CXCL9, CXCL10, CXCR3 and PD-1[39].

The relationships between significant DEGs expression and the OS of LUAD patients were then evaluated by K-M plotter. The up-regulation of C3AR1 and CCR5 were associated with high OS rates, while the down-regulation of FPR2 and MCHR1 were related to poor OS rates. These 4 OS-related genes are defined as hub genes. Furthermore, we investigated the correlations between the hub genes and immune infiltration. C3AR1 and CCR5 were positively correlated with immune cell infiltration, including B cells, CD4 + T cells, CD8 + T cells, macrophages, neutrophils, and dendritic cells. FPR2 and MCHR1 were positively correlated with few immune cell infiltration. Previous studies showed that CD4 + T cells, CD8 + T cells and macrophages played important roles in the TME and tumor prognosis. In pancreatic tumor tissues, the higher proportions of CD4 + and CD8 + T cells, the better long-term prognosis for patients[40]. In breast carcinoma, annexin1 promoted polarization of M1 macrophages and induced pro-inflammatory genes[41]. Nevertheless, it was reported that the higher numbers of T or B cells, the worse capsular and perineural invasion in prostate cancer[42].

We also proved that LYN, LCK and SYK were the mutual kinase targets of the hub genes. It was reported that down-regulation of LYN inhibited the proliferation, migration and invasion of melanoma cell lines via suppressing PI3K/AKT signaling pathway[43]. Combined treatment of SYK inhibitor and PI3K inhibitor induced anti-tumor immune responses via promoting pro-inflammatory macrophage phenotype and activating CD8 + T cells[44]. LCK was also reported to activate T cell via facilitating costimulatory molecule CD28-mediated signal transduction and LAT phosphorylation[45].

There are several limitations in our current study. First, this study was mainly based on publicly accessible big-data applying the computational-biology algorithm. Second, the intrinsic mechanisms of between these hub-genes and immune cell infiltration remained unclear.

In summary, we identified 4 survival-related hub genes, FPR2, C3AR1, CCR5 and MCHR1. Their kinase targets might be used for immune-combined therapy. Our studies provided new perspectives on LUAD immunotherapy.

Conclusions

Four hub genes, FPR2, C3AR1, CCR5 and MCHR1, were significantly associated with the prognosis and immune cell infiltration in LUAD. LYN, LCK and SYK were the mutual kinase targets of these hub genes. Our researches enhanced TME-related gene features and provided novel immune targets for clinical researches.

Abbreviations

LUAD: lung adenocarcinoma; TME: tumor microenvironment; TCGA: the cancer genome atlas; DEGs: differentially expressed genes; PPI: protein-protein interaction; K-M: Kaplan-Meier; GO: Gene Ontology; KEGG: Kyoto Encyclopedia of Genes and Genomes; OS: overall survival; NSCLC: non-small cell lung cancer; FDR: false discovery rate; BPs: biological processes; MFs: molecular functions; CCs: cellular components; CAMs: cell adhesion molecules. FC: fold change.

Declarations

Ethics approval and consent to participate

Not applicable.

Consent for publication

Not applicable.

Availability of data and materials

The datasets during and/or analyzed during the current study available from the corresponding author on reasonable request.

Competing interests

The authors declare that they have no competing interests.

Funding

This study was supported by National Natural Science Foundation of China (81773236, 81800429 and 81972852), the Fundamental Research Funds for the Central Universities (2042018kf0065, 2042018kf1037, and 2042019kf0329), Health Commission of Hubei Province Medical Leading Talent Project, Health Commission of Hubei Province Scientific Research Project (WJ2019H002 and WJ2019Q047), Young and Middle-Aged Medical Backbone Talents of Wuhan (WHQG201902), Medical Science Advancement Program (Basic Medical Sciences) of Wuhan University (TFJC2018005), and Zhongnan Hospital of Wuhan University Science, Technology and Innovation Seed Fund (znpy2017001, znpy2017049, znpy2018028 and znpy2019070).

Authors' contributions

XJ, YG and CX designed the study. XJ, YG, NZ and CY collected the mRNA transcriptome data and clinical information from TCGA. XJ, YL, WS and JZ performed statistical analyses. XJ and JR wrote the manuscript. YG and CX improved and revised the manuscript. All authors read and approved the final manuscript.

Acknowledgements

None.

References

1. Bray F, Ferlay J, Soerjomataram I, Siegel RL, Torre LA, Jemal A. Global cancer statistics 2018: GLOBOCAN estimates of incidence and mortality worldwide for 36 cancers in 185 countries. CA Cancer J Clin. 2018;68(6):394-424.
2. Herbst RS, Morgensztern D, Boshoff C. The biology and management of non-small cell lung cancer. Nature. 2018;553(7689):446-54.
3. Osmani L, Askin F, Gabrielson E, Li QK. Current WHO guidelines and the critical role of immunohistochemical markers in the subclassification of non-small cell lung carcinoma (NSCLC): Moving from targeted therapy to immunotherapy. Semin Cancer Biol. 2018;52:103-09.
4. Wu T, Dai Y. Tumor microenvironment and therapeutic response. Cancer Lett. 2017;387:61-68.
5. Gao Y, Khan GJ, Wei X, Zhai KF, Sun L, Yuan S. DT-13 inhibits breast cancer cell migration via non-muscle myosin II-A regulation in tumor microenvironment synchronized adaptations. Clin Transl Oncol. 2020. https://doi.org/10.1007/s12094-020-02303-z.
6. Margolin DA, Silinsky J, Grimes C, Spencer N, Aycock M, Green H, et al. Lymph node stromal cells enhance drug-resistant colon cancer cell tumor formation through SDF-1alpha/CXCR4 paracrine signaling. Neoplasia. 2011;13(9):874-86.
7. Chen Y, Jacamo R, Konopleva M, Garzon R, Croce C, Andreeff M. CXCR4 downregulation of let-7a drives chemoresistance in acute myeloid leukemia. J Clin Invest. 2013;123(6):2395-407.
8. Xu H, Hu M, Liu M, An S, Guan K, Wang M, et al. Nano-puerarin regulates tumor microenvironment and facilitates chemo- and immunotherapy in murine triple negative breast cancer model. Biomaterials. 2020;235:119769.
9. Zhang W, Hu X, Liang J, Zhu Y, Zeng B, Feng L, et al. oHSV2 Can Target Murine Colon Carcinoma by Altering the Immune Status of the Tumor Microenvironment and Inducing Antitumor Immunity. Mol Ther Oncolytics. 2020;16:158-71.
10. Zhou Q, Bauden M, Andersson R, Hu D, Marko-Varga G, Xu J, et al. YAP1 is an independent prognostic marker in pancreatic cancer and associated with extracellular matrix remodeling. J Transl Med. 2020;18(1):77.
11. Yoshihara K, Shahmoradgoli M, Martinez E, Vegesna R, Kim H, Torres-Garcia W, et al. Inferring tumour purity and stromal and immune cell admixture from expression data. Nat Commun. 2013;4:2612.

12. Jia D, Li S, Li D, Xue H, Yang D, Liu Y. Mining TCGA database for genes of prognostic value in glioblastoma microenvironment. Aging (Albany NY). 2018;10(4):592-605.
13. Zeng Q, Zhang W, Li X, Lai J, Li Z. Bioinformatic identification of renal cell carcinoma microenvironment-associated biomarkers with therapeutic and prognostic value. Life Sci. 2020;243:117273.
14. Tomczak K, Czerwinska P, Wiznerowicz M. The Cancer Genome Atlas (TCGA): an immeasurable source of knowledge. Contemp Oncol (Pozn). 2015;19(1A):A68-77.
15. Ritchie ME, Phipson B, Wu D, Hu Y, Law CW, Shi W, Smyth GK. limma powers differential expression analyses for RNA-sequencing and microarray studies. Nucleic Acids Res. 2015;43(7):e47.
16. Galili T, O'Callaghan A, Sidi J, Sievert C. heatmaply: an R package for creating interactive cluster heatmaps for online publishing. Bioinformatics. 2018;34(9):1600-02.
17. Chen H, Boutros PC. VennDiagram: a package for the generation of highly-customizable Venn and Euler diagrams in R. Bmc Bioinformatics. 2011;12:35.
18. Yu G, Wang LG, Han Y, He QY. clusterProfiler: an R package for comparing biological themes among gene clusters. Omics. 2012;16(5):284-87.
19. Szklarczyk D, Gable AL, Lyon D, Junge A, Wyder S, Huerta-Cepas J, et al. STRING v11: protein-protein association networks with increased coverage, supporting functional discovery in genome-wide experimental datasets. Nucleic Acids Res. 2019;47(D1):D607-13.
20. Gyorffy B, Surowiak P, Budczies J, Lanczky A. Online survival analysis software to assess the prognostic value of biomarkers using transcriptomic data in non-small-cell lung cancer. Plos One. 2013;8(12):e82241.
21. Li T, Fan J, Wang B, Traugh N, Chen Q, Liu JS, Li B, Liu XS. TIMER: A Web Server for Comprehensive Analysis of Tumor-Infiltrating Immune Cells. Cancer Res. 2017;77(21):e108-10.
22. Vasaikar SV, Straub P, Wang J, Zhang B. LinkedOmics: analyzing multi-omics data within and across 32 cancer types. Nucleic Acids Res. 2018;46(D1):D956-63.
23. Inamura K. Clinicopathological Characteristics and Mutations Driving Development of Early Lung Adenocarcinoma: Tumor Initiation and Progression. Int J Mol Sci. 2018;19(4)
24. Kris MG, Johnson BE, Berry LD, Kwiatkowski DJ, Iafrate AJ, Wistuba II, et al. Using multiplexed assays of oncogenic drivers in lung cancers to select targeted drugs. JAMA. 2014;311(19):1998-2006.
25. Shaw AT, Kim DW, Mehra R, Tan DS, Felip E, Chow LQ, et al. Ceritinib in ALK-rearranged non-small-cell lung cancer. N Engl J Med. 2014;370(13):1189-97.
26. Futosi K, Fodor S, Mocsai A. Neutrophil cell surface receptors and their intracellular signal transduction pathways. Int Immunopharmacol. 2013;17(3):638-50.
27. Tan Q, Huang Y, Deng K, Lu M, Wang L, Rong Z, et al. Identification immunophenotyping of lung adenocarcinomas based on the tumor microenvironment. J Cell Biochem. 2020.https://doi.org/10.1002/jcb.29675

28. Angel PM, Bruner E, Bethard J, Clift CL, Ball L, Drake RR, Feghali-Bostwick C. Extracellular Matrix Alterations in Low Grade Lung Adenocarcinoma Compared to Normal Lung Tissue by Imaging Mass Spectrometry. J Mass Spectrom. 2020;e4450.https://doi.org/10.1002/jms.4450.
29. Wang W, Ren S, Wang Z, Zhang C, Huang J. Increased expression of TTC21A in lung adenocarcinoma infers favorable prognosis and high immune infiltrating level. Int Immunopharmacol. 2020;78:106077.
30. Liu Y, Chen K, Wang C, Gong W, Yoshimura T, Liu M, Wang JM. Cell surface receptor FPR2 promotes antitumor host defense by limiting M2 polarization of macrophages. Cancer Res. 2013;73(2):550-60.
31. Hou XL, Ji CD, Tang J, Wang YX, Xiang DF, Li HQ, et al. FPR2 promotes invasion and metastasis of gastric cancer cells and predicts the prognosis of patients. Sci Rep. 2017;7(1):3153.
32. Lu J, Zhao J, Jia C, Zhou L, Cai Y, Ni J, Ma J, Zheng M, Lu A. FPR2 enhances colorectal cancer progression by promoting EMT process. Neoplasma. 2019;66(5):785-91.
33. Mathern DR, K HJ, Heeger PS. Absence of recipient C3aR1 signaling limits expansion and differentiation of alloreactive CD8(+) T cell immunity and prolongs murine cardiac allograft survival. Am J Transplant. 2019;19(6):1628-40.
34. Shu C, Zha H, Long H, Wang X, Yang F, Gao J, et al. C3a-C3aR signaling promotes breast cancer lung metastasis via modulating carcinoma associated fibroblasts. J Exp Clin Cancer Res. 2020;39(1):11.
35. Jiao X, Nawab O, Patel T, Kossenkov AV, Halama N, Jaeger D, Pestell RG. Recent Advances Targeting CCR5 for Cancer and Its Role in Immuno-Oncology. Cancer Res. 2019;79(19):4801-07.
36. Vacchelli E, Ma Y, Baracco EE, Sistigu A, Enot DP, Pietrocola F, et al. Chemotherapy-induced antitumor immunity requires formyl peptide receptor 1. Science. 2015;350(6263):972-78.
37. Cheng HW, Onder L, Cupovic J, Boesch M, Novkovic M, Pikor N, et al. CCL19-producing fibroblastic stromal cells restrain lung carcinoma growth by promoting local antitumor T-cell responses. J Allergy Clin Immunol. 2018;142(4):1257-71.
38. Li X, Yao W, Yuan Y, Chen P, Li B, Li J, et al. Targeting of tumour-infiltrating macrophages via CCL2/CCR2 signalling as a therapeutic strategy against hepatocellular carcinoma. Gut. 2017;66(1):157-67.
39. K AK, Peterson N, Truesdell P, Reid-Schachter G, Khalaj K, Ren R, et al. CXCL10 alters the tumour immune microenvironment and disease progression in a syngeneic murine model of high-grade serous ovarian cancer. Gynecol Oncol. 2017;145(3):436-45.
40. Ren B, Cui M, Yang G, Wang H, Feng M, You L, Zhao Y. Tumor microenvironment participates in metastasis of pancreatic cancer. Mol Cancer. 2018;17(1):108.
41. Mittal S, Brown NJ, Holen I. The breast tumor microenvironment: role in cancer development, progression and response to therapy. Expert Rev Mol Diagn. 2018;18(3):227-43.
42. Shiao SL, Chu GC, Chung LW. Regulation of prostate cancer progression by the tumor microenvironment. Cancer Lett. 2016;380(1):340-48.

43. Zhang Q, Meng X, Qin G, Xue X, Dang N. Lyn Kinase Promotes the Proliferation of Malignant Melanoma Cells through Inhibition of Apoptosis and Autophagy via the PI3K/Akt Signaling Pathway. J Cancer. 2019;10(5):1197-208.
44. Joshi S, Liu KX, Zulcic M, Singh AR, Skola D, Glass CK, et al. Macrophage Syk-PI3Kgamma inhibits anti-tumor immunity: SRX3207, a novel dual Syk-PI3K inhibitory chemotype relieves tumor immunosuppression. Mol Cancer Ther. 2020;19(3):755-64.
45. Bommhardt U, Schraven B, Simeoni L. Beyond TCR Signaling: Emerging Functions of Lck in Cancer and Immunotherapy. Int J Mol Sci. 2019;20(14):3500.

Additional Files

Figure S1. Association between the OS and FPR1, CCL19, CCR2 and CXCL10 in LUAD patients.

Figure S2. Identification of mutual kinase targets of hub genes by Venn diagram.

Table S1. Identification of the up- and downregulated DEGs in LUAD.

Figures

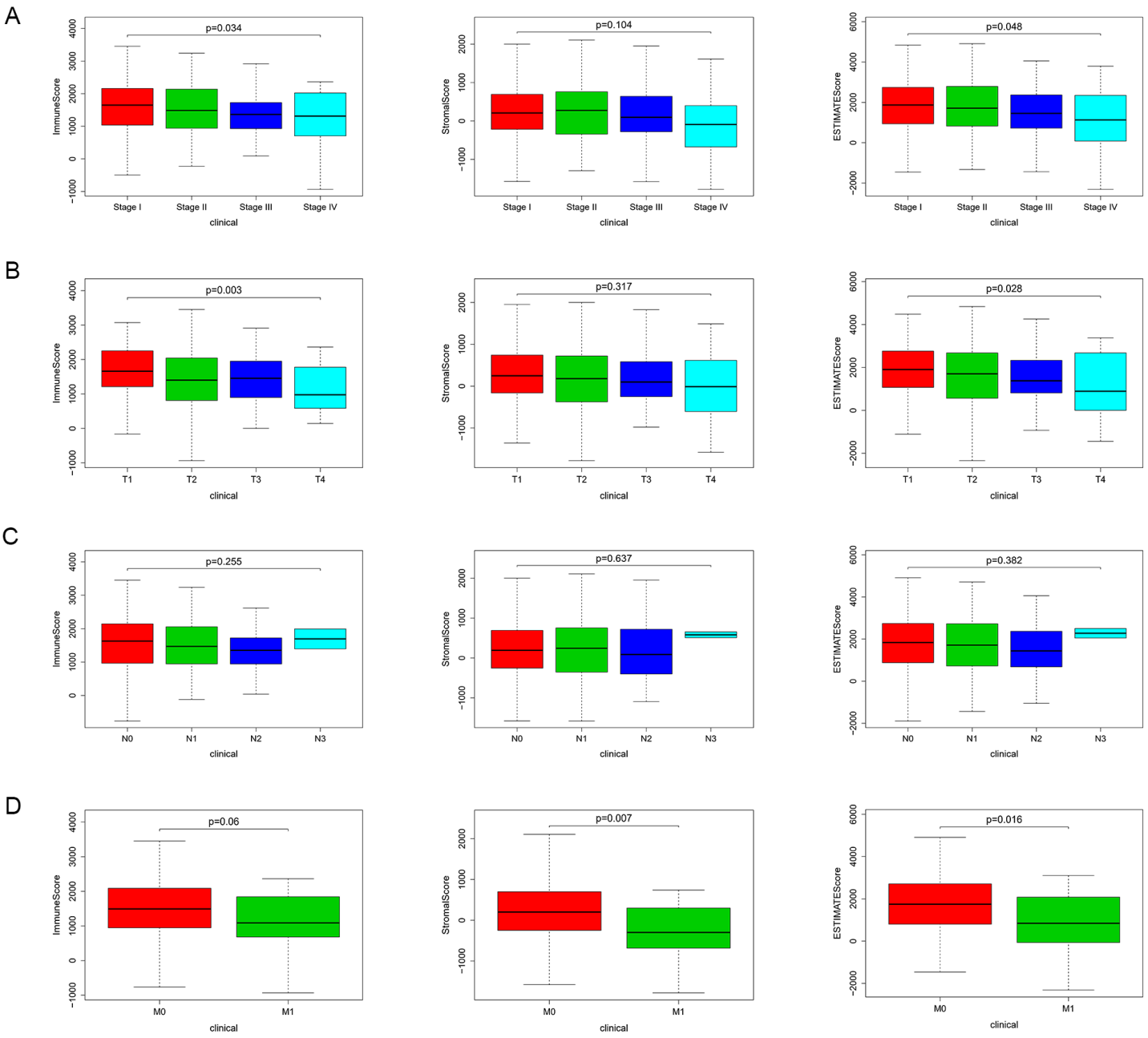

Figure 1

The relationships between immune/stromal scores and malignant progression in LUAD. (A) High tumor stages were significantly associated with low immune scores (P = 0.034) and low ESTIMATE scores (P = 0.048). (B) Larger sizes of tumor were significantly associated with low immune scores (P = 0.003) and low ESTIMATE scores (P = 0.028). (C) There was no statistically significant difference between lymph node metastases and immune scores (P = 0.255), stromal scores (P = 0.637), or ESTIMATE scores (P = 0.382). (D) Distant metastasis was significantly associated with low stromal scores (P = 0.007) and low ESTIMATE scores (P = 0.016).

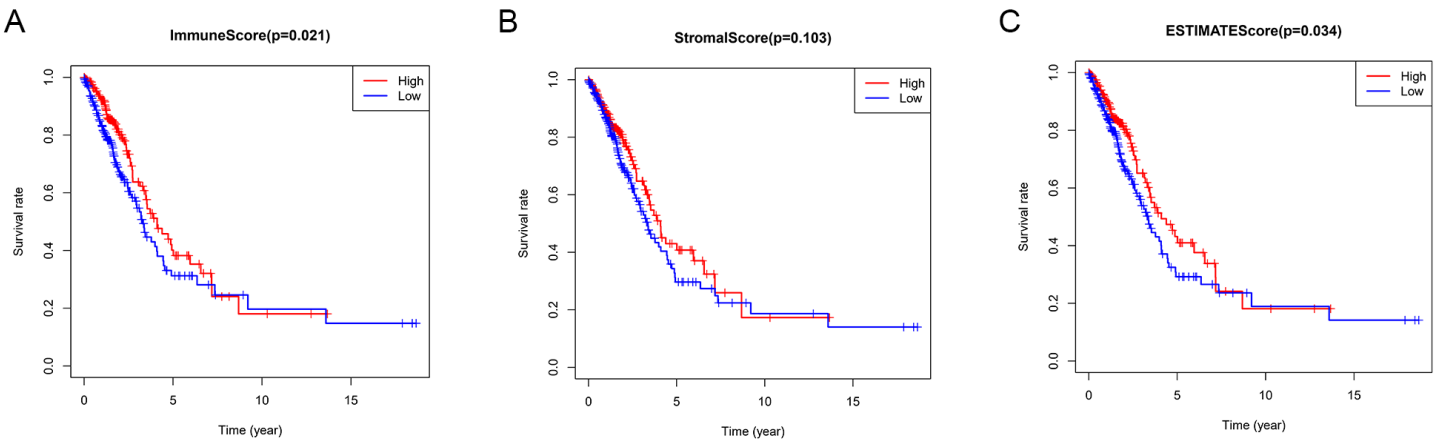

Figure 2

The relationships between the immune/stromal scores and OS of LUAD patients. (A) The immune scores were negatively related with the OS of patients (P = 0.021). (B) No statistically significant difference between the stromal scores and the OS of patients (P = 0.103). (C) The ESTIMATE scores were negatively correlated with the OS of patients (P = 0.034). The p-value was calculated using the log-rank test.

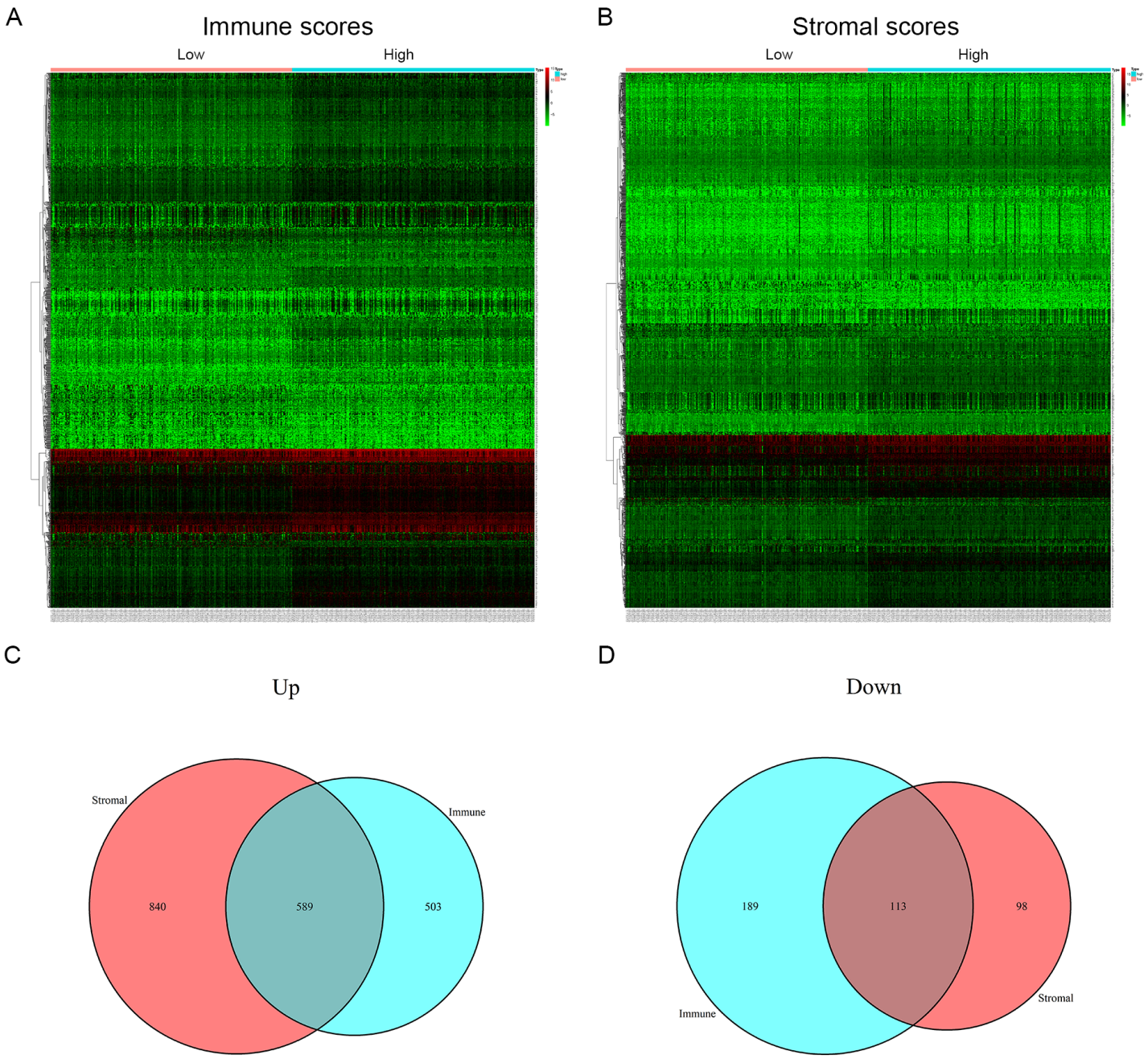

Figure 3

Gene expression profiles of immune/stromal scores in LUAD. (A, B) Heatmaps of gene expressions between the high and low immune/stromal score groups. FC > 2 and p < 0.05 were considered as criterion. (C, D) The numbers of up- or down-regulated genes in the stromal and immune score groups in Venn diagrams. Heatmaps were displayed on the basis of the average linkage and Pearson distance measurement method.

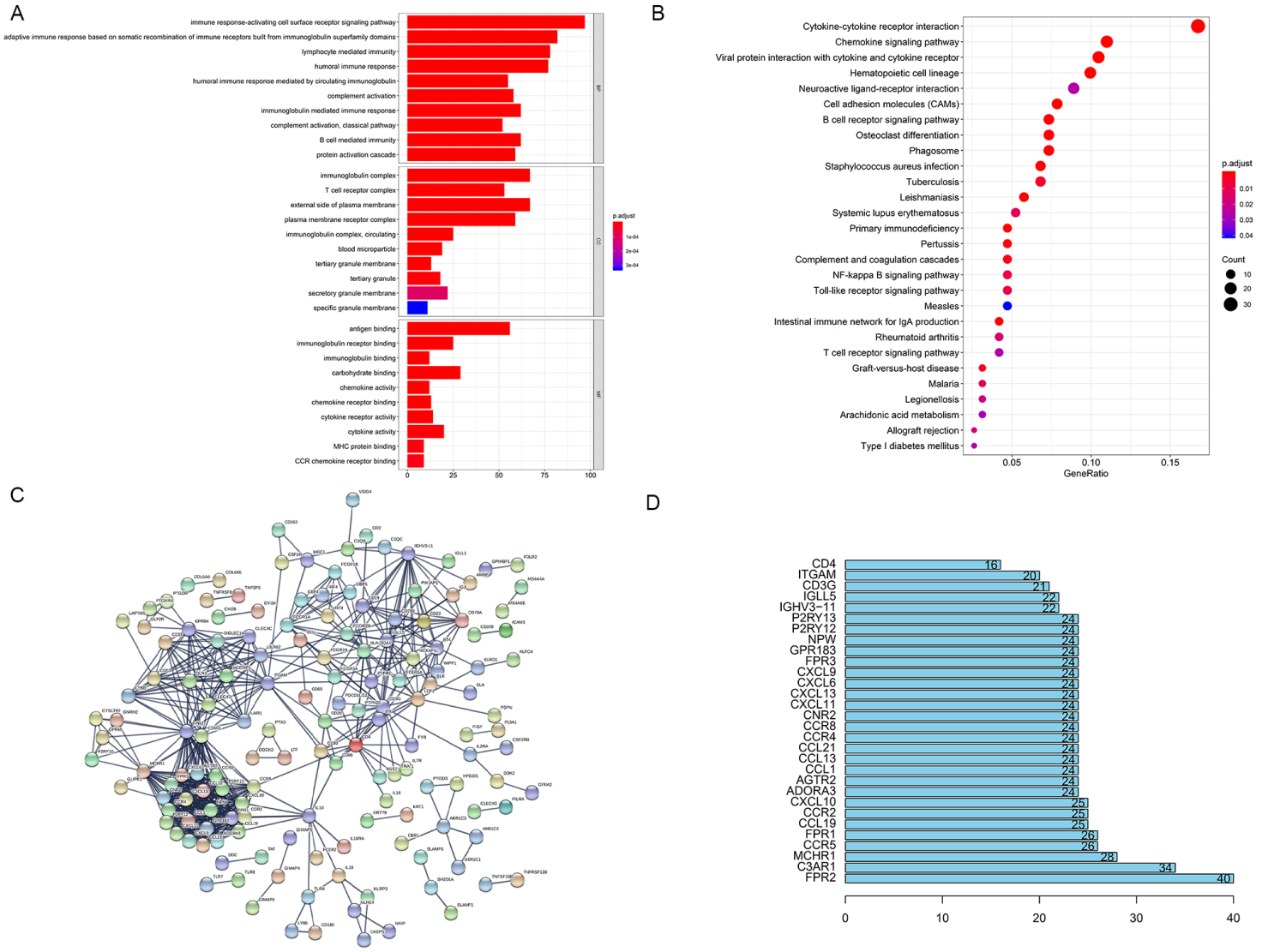

Figure 4

GO, KEGG and PPI network. (A) Top 10 terms (BPs, MFs, CCs) in GO analysis were represented in the Bar plot. (B) Bubble chart showing the enriched signal pathways in KEGG analysis. (C) PPI network was shown using the STRING tool. The median confidence interval was set as 0.9. (D) The significant genes in the PPI network were exhibited in the Bar plot. P < 0.05 was considered as statistical significance.

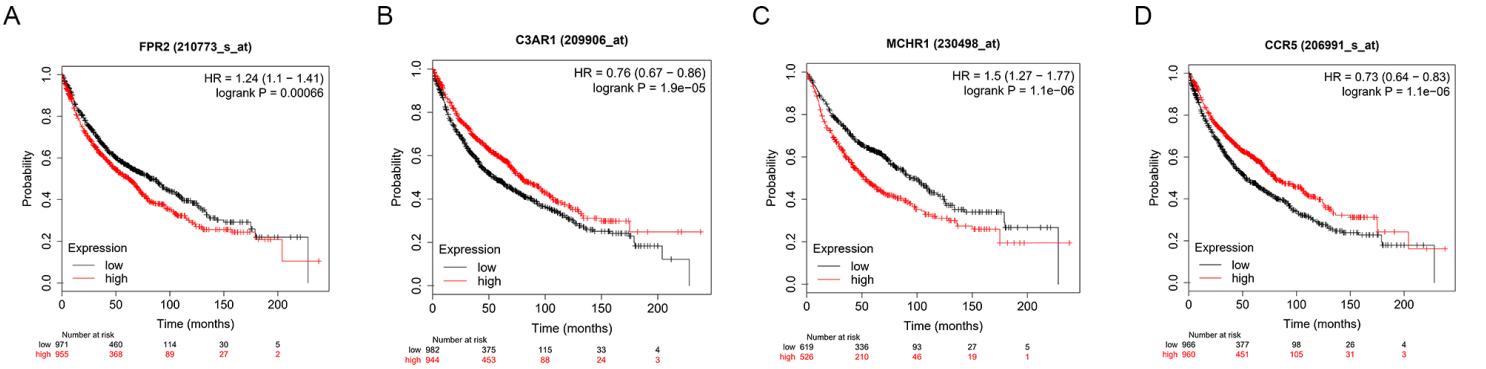

Figure 5

Using the K-M Plotter online tool, OS analyses of hub genes (FPR2, C3AR1, MCHR1 and CCR5) were showed. P < 0.05 was considered as statistical significance.

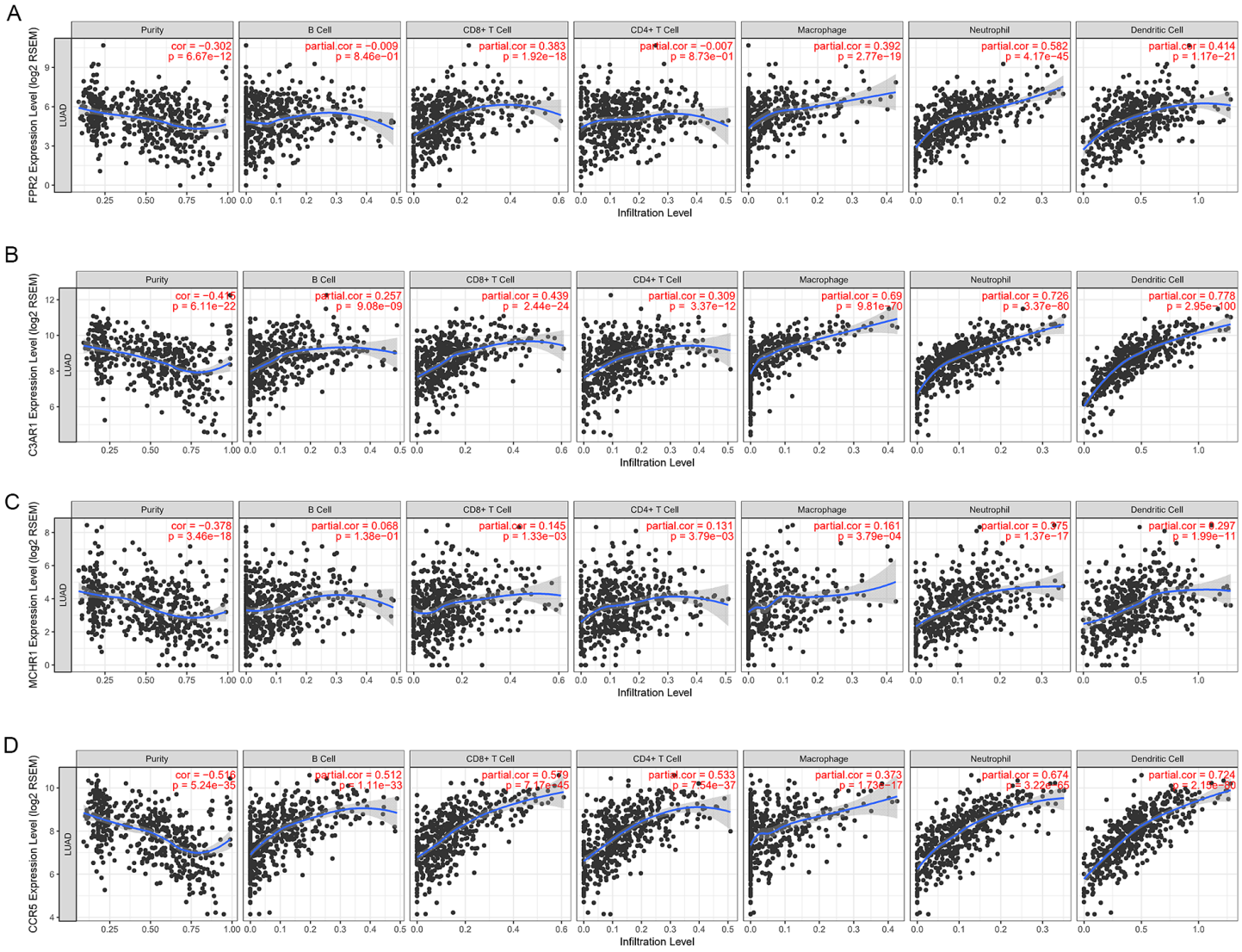

Figure 6

Associations of the hub genes and various immune cells. (A) The expression levels of FPR2 were significantly associated with the degree of immune cell infiltration, including CD8+ T cells, macrophages, neutrophils, and dendritic cells. (B) The expression levels of C3AR1 were significantly associated with the degree of immune cell infiltration, including B cells, CD4+ T cells, CD8+ T cells, macrophages, neutrophils, and dendritic cells. (C) The expression levels of MCHR1 were significantly associated with the degree of immune cell infiltration, including CD4+ T cells, CD8+ T cells, macrophages, neutrophils, and dendritic cells. (D) The expression levels of CCR5 were significantly associated with the degree of immune cell infiltration, including B cells, CD4+ T cells, CD8+ T cells, macrophages, neutrophils, and dendritic cells.

Supplementary Files

This is a list of supplementary files associated with this preprint. Click to download.

- Additionalfile3.tif
- Additionalfile2.tif
- Additionalfile1.xlsx